Density-scaling exponents and virial potential-energy correlation coefficients for the $(2n, n)$ Lennard-Jones system

Ida M. Friisberg,[*] Lorenzo Costigliola,[†] and Jeppe C. Dyre[‡]

Glass and Time, IMFUFA, Department of Science and Environment,
Roskilde University, P.O. Box 260, DK-4000 Roskilde, Denmark

(Dated: January 20, 2017)

This paper investigates the relation between the density-scaling exponent γ and the virial potential-energy correlation coefficient R at several thermodynamic state points in three dimensions for the generalized $(2n, n)$ Lennard-Jones (LJ) system for $n = 4, 9, 12, 18$, as well as for the standard $n = 6$ LJ system in two, three, and four dimensions. The state points studied include many low-density states at which the virial potential-energy correlations are not strong. For these state points we find the roughly linear relation $\gamma \cong 3nR/d$ in d dimensions. This result is discussed in light of the approximate "extended inverse power law" description of generalized LJ potentials [N. P. Bailey *et al.*, J. Chem. Phys. **129**, 184508 (2008)]. In the plot of γ versus R there is in all cases a transition around $R \approx 0.9$, above which γ starts to decrease as R approaches unity. This is consistent with the fact that $\gamma \to 2n/d$ for $R \to 1$, a limit that is approached at high densities and/or temperatures at which the repulsive r^{-2n} term dominates the physics.

---

[*] idafriisberg@gmail.com
[†] lorenzo.costigliola@gmail.com
[‡] dyre@ruc.dk

I. INTRODUCTION

In the past decade a class of systems has been identified that is well described by the isomorph theory [1–8], sometimes referred to as R (Roskilde) simple systems [9–18]. This class is believed to include most van der Waals bonded and metallic liquids and solids, as well as most weakly dipolar or ionic systems. The class, on the other hand, does not include systems with strong directional bonds like hydrogen or covalently bonded systems [8].

To determine whether the isomorph theory holds for a given system one calculates the strength of the virial potential-energy correlations in NVT simulations, i.e., in the canonical ensemble [1, 2]. Isomorphs are curves of invariant structure and dynamics in the thermodynamic phase diagram, see Sec. II A. A system has isomorphs if and only if it has strong virial potential-energy correlations [4]. Virial potential-energy correlations are quantified by the state-point dependent Pearson correlation coefficient R defined as

$$R\left(\rho, T\right) = \frac{\langle \Delta W \Delta U \rangle}{\sqrt{\langle (\Delta W)^2 \rangle \langle (\Delta U)^2 \rangle}} \, . \tag{1}$$

In Eq. (1) ρ is the (number) density ($\rho = N/V$ with N particles in volume V), T is the temperature, W and U are the virial and potential energy, the brackets denote NVT averages, and Δ is the instantaneous deviation from equilibrium.

The isomorph theory is exact only for systems with a potential that is a constant plus an Euler-homogeneous function, in which case the correlation coefficient R in Eq. (1) is unity for all ρ and T [4]. An example is the inverse-power-law (IPL) pair-potential systems. For non-Euler-homogeneous potentials, which includes all realistic systems, the quantity R is less than unity. In that case the applicability of the isomorph theory is restricted to a certain region of the phase diagram, usually the condensed-phase region encompassing the solid and "ordinary" liquid phase.

A system is defined to be R simple whenever $R > 0.9$ [1], because this ensures that isomorphs exist to a good approximation [4]. The $R = 0.9$ threshold is somewhat arbitrary, however. The present paper investigates what happens when R falls below the threshold. From the isomorph theory there is little help, because it generally breaks down when correlations are no longer strong, i.e., when the correlation coefficient goes significantly below 0.9 [2, 4, 7]. In 2014, however, an interesting paper appeared by Prasad and Chakravarty [13] establishing that Rosenfeld's excess entropy scaling as well as density-scaling [19], which may both be derived from the isomorph theory [4], need not break down even if the virial potential-energy correlations are weak. Reference 13 studied the transition to simple liquid behavior in computer simulations of modified water models. We have taken inspiration from this work to systematically study the region of phase space where virial potential-energy correlations are not strong, but here for a class of models that – in contrast to water models – do have sizable regions of strong correlations in the thermodynamic phase diagram. This is done by studying Lennard-Jones type systems at lower densities than have previously been in focus.

This paper presents a study of the LJ$(2n, n)$ class of potentials defined as single-component systems with LJ-type radially symmetric pair potentials with a repulsive term proportional to r^{-2n} and an attractive term proportional to r^{-n} (r is the interparticle distance). Results are presented for the cases $n = 4, 9, 12, 18$ in three dimensions, as well as for the standard LJ potential ($n = 6$) in two, three, and four spatial dimensions (Sec. III). Before doing this the isomorph theory is briefly reviewed (Sec. II A). Section IV summarizes the paper's findings.

II. THEORETICAL/COMPUTATIONAL

A. Aspects of the isomorph theory

R simple systems – previously termed "strongly correlating" which, however, led to confusion with strongly correlated quantum systems – were in 2009 defined by reference to strong virial potential-energy correlations [1]. This section presents the alternative definition of the same class of systems from 2014 [14] that refers to their "hidden scale invariance" [7]. The original formulation of the isomorph theory [4] is recovered via a first-order Taylor expansion [14].

Consider an N-particle system in d spatial dimensions. The system is defined to be R simple if for any two configurations corresponding to the same density that obey $U(\mathbf{R}_a) < U(\mathbf{R}_b)$, this ordering is preserved after a uniform scaling of the two configurations [14] ($\mathbf{R}$ is the dN dimensional vector describing a configuration of N particles in d spatial dimensions). Formally, this condition is written [14]

$$U\left(\mathbf{R}_{\mathrm{a}}\right) < U\left(\mathbf{R}_{\mathrm{b}}\right) \Rightarrow U\left(\lambda\mathbf{R}_{\mathrm{a}}\right) < U\left(\lambda\mathbf{R}_{\mathrm{b}}\right) . \qquad (2)$$

In computer simulations periodic boundary conditions are applied, and it is understood that the box size scales with $\mathbf{R}$. Equation (2) need not be obeyed for all configurations; as long as it applies for most of the physically relevant configurations, the predictions of isomorph theory are obeyed to a good approximation.

In Eq. (2) the scaling factor λ can be any positive real number, and the equation holds for scaling "both ways". Because of this an R simple system obeys [14]

$$U\left(\mathbf{R}_{\mathrm{a}}\right) = U\left(\mathbf{R}_{\mathrm{b}}\right) \Rightarrow U\left(\lambda\mathbf{R}_{\mathrm{a}}\right) = U\left(\lambda\mathbf{R}_{\mathrm{b}}\right) . \qquad (3)$$

Thus if two configurations have the same potential energy, their scaled potential energies are also identical.

R simple systems are characterized by strong correlations between virial and potential-energy fluctuations in the NVT ensemble. This can be derived from Eq. (3) in the following way. For two configurations, $\mathbf{R}_1$ and $\mathbf{R}_2$, at the same density with the same potential energy, Eq. (3) states that $U(\lambda\mathbf{R}_1) = U(\lambda\mathbf{R}_2)$. Taking the derivative of this identity with respect to λ one obtains

$$\mathbf{R}_1 \cdot \nabla U(\lambda\mathbf{R}_1) = \mathbf{R}_2 \cdot \nabla U(\lambda\mathbf{R}_2) . \qquad (4)$$

Using the definition of virial $W(\mathbf{R}) \equiv \mathbf{R} \cdot \nabla\mathbf{U}(\mathbf{R})/d$ [20], one gets for $\lambda = 1$

$$W(\mathbf{R}_1) = W(\mathbf{R}_2) . \qquad (5)$$

Thus $U(\mathbf{R})$ determines $W(\mathbf{R})$, implying perfect correlation. This applies for systems that satisfy Eq. (2) or, equivalently Eq. (3), for all configurations; it holds for realistic R simple systems to a good approximation. As a consequence, for such systems the correlation coefficient R of Eq. (1) is close to unity, but not exactly unity. As mentioned, the threshold defining R simple systems has usually been taken to be $R = 0.9$ [1].

Two configurations of density ρ_1 and ρ_2, which scale uniformly into one another, i.e., $\mathbf{R}_2 = \lambda\mathbf{R}_1$ for some λ, are related through the following equality (where d is the dimension):

$$\rho_1^{1/d}\boldsymbol{R}_1 = \rho_2^{1/d}\boldsymbol{R}_2 \equiv \tilde{\boldsymbol{R}} . \qquad (6)$$

The last equality defines the "reduced" (dimensionless) configuration vector $\tilde{\mathbf{R}}$. Henceforth reduced quantities are marked by a tilde. The reduced version of a physical quantity is obtained by using the "macroscopic" unit system in which the length unit is $\rho^{-1/d}$, the energy unit is $k_B T$, and the time unit is $\rho^{-1/d}/\sqrt{mk_B T}$ (m is the particle mass) [21].

The entropy of any physical system can be written as an ideal-gas term plus an excess term S_{ex}. The ideal-gas term is the entropy of an ideal gas at the density and temperature in question, the excess term is the contribution to entropy from the interactions between the particles. We define the microscopic excess entropy function, $S_{\mathrm{ex}}(\mathbf{R})$, to be the thermodynamic excess entropy [14, 22] of the potential-energy surface the configuration belongs to, i.e.,

$$S_{\mathrm{ex}}(\boldsymbol{R}) \equiv S_{\mathrm{ex}}\left(\rho, U\left(\boldsymbol{R}\right)\right) . \qquad (7)$$

The function on the right-hand side, $S_{\mathrm{ex}}\left(\rho, U\right)$, is the *thermodynamic* excess entropy of the state point with density ρ and average potential energy $U(\mathbf{R})$. In other words, the microscopic excess entropy of a configuration $\mathbf{R}$ is defined as the excess entropy of a thermodynamic equilibrium system of same density with average energy precisely equal to $U(\boldsymbol{R})$.

Inverting Eq. (7) we get

$$U\left(\boldsymbol{R}\right) = U\left(\rho, S_{\mathrm{ex}}\left(\boldsymbol{R}\right)\right) \qquad (8)$$

in which the function on the right-hand side, $U\left(\rho, S_{\mathrm{ex}}\right)$, is the thermodynamic average potential energy of the state point with density ρ and excess entropy S_{ex}.

Equations (7) and (8) apply for any system [22], but they are particularly significant for R simple systems for which they imply that the configurational adiabats are curves of invariant structure and dynamics. To prove this, we first note that, as shown in Ref. 14, Eq. (2) implies that the excess-entropy function is invariant under uniform scaling, i.e., it only depends on the reduced coordinate vector $\tilde{\mathbf{R}}$:

$$S_{\text{ex}}(\boldsymbol{R}) = S_{\text{ex}}(\tilde{\boldsymbol{R}}). \tag{9}$$

The relation for the potential-energy function Eq. (8) consequently becomes

$$U(\boldsymbol{R}) = U(\rho, S_{\text{ex}}(\tilde{\boldsymbol{R}})). \tag{10}$$

Isomorphs are defined as the configurational adiabats, i.e., curves along which the excess entropy is constant, in the region of phase diagram where the system is R simple [4]. To demonstrate invariance of structure and dynamics along the isomorphs we show that Newton's second law in reduced units is invariant along an isomorph. In complete generality, this law is in reduced units (note that the particle mass is absorbed into the reduced time)

$$\frac{d^2 \tilde{\boldsymbol{R}}}{d\tilde{t}^2} = \frac{\rho^{-1/d}}{k_B T} \boldsymbol{F}(\boldsymbol{R}) \equiv \tilde{\boldsymbol{F}}(\boldsymbol{R}). \tag{11}$$

For R simple systems Eq. (10) implies

$$\boldsymbol{F} = -\nabla U = -\left(\frac{\partial U}{\partial S_{\text{ex}}}\right)_\rho \nabla S_{\text{ex}}(\tilde{\boldsymbol{R}}). \tag{12}$$

Using $\nabla = \rho^{1/d}\tilde{\nabla}$ and $(\partial U/\partial S_{\text{ex}})_\rho = T$, the above expression becomes

$$\boldsymbol{F} = -\rho^{1/d} T \tilde{\nabla} S_{\text{ex}}(\tilde{\boldsymbol{R}}) \tag{13}$$

or

$$\tilde{\boldsymbol{F}} = -\frac{\tilde{\nabla} S_{\text{ex}}(\tilde{\boldsymbol{R}})}{k_B}. \tag{14}$$

This expression reveals that for R simple systems the reduced force $\tilde{\boldsymbol{F}}$ is a function of the reduced coordinate vector, implying that Eq. (11) is invariant along an isomorph. Thus structure and dynamics in reduced units are isomorph invariant [14].

B.   The density-scaling exponent

When strong correlations between virial and potential energy are present, a constant of proportionality between the instantaneous fluctuations of these two quantities' deviation from their equilibrium values, γ, can be introduced via

$$\Delta W(t) \simeq \gamma \Delta U(t). \tag{15}$$

The correlation coefficient associated with this linear regression is that given in Eq. (1). The exact definition of γ is the following [4]:

$$\gamma = \frac{\langle \Delta W \Delta U \rangle}{\langle (\Delta U)^2 \rangle}. \tag{16}$$

By applying a standard fluctuation relation and the volume-temperature Maxwell relation one can show [4] that

$$\gamma = \left(\frac{\partial \ln T}{\partial \ln \rho} \right)_{S_{\mathrm{ex}}} . \tag{17}$$

The number γ is termed the density-scaling exponent [4, 19]. It determines the configurational adiabats, which are isomorphs in the R simple region of the phase diagram. If variations of γ may be ignored, these curves are via Eq. (17) given by $\rho^{\gamma}/T = \mathrm{Const}$. In the general case, Eq. (17) can be used to trace out isomorphs step-by-step by repeatedly changing density by typically an amount of order 1%, calculating the temperature change via Eq. (17), recalculating γ from Eq. (16) at the new state point, etc.

In early publications [1, 2] we identified the constant of proportionality γ of Eq. (15) by the following symmetric fluctuation expression, which was later renamed γ_2 to distinguish it from γ [4]:

$$\gamma_2 = \sqrt{\frac{\langle (\Delta W)^2 \rangle}{\langle (\Delta U)^2 \rangle}} . \tag{18}$$

Whenever the correlation coefficient R is close to unity, one has $\gamma \cong \gamma_2$ since the following applies

$$\gamma = \gamma_2 \, R . \tag{19}$$

Now that the main ingredients of the isomorph theory have been introduced, we proceed to present the simulation results.

III.   RESULTS AND DISCUSSION

A.   Generalized Lennard-Jones pair potentials in three dimensions

If r is the interparticle distance, the generalized LJ pair potential is defined as follows

$$v_{m,n}^{\mathrm{LJ}}(r) = \frac{\varepsilon}{m-n} \left[n \left(\frac{\sigma}{r} \right)^{m} - m \left(\frac{\sigma}{r} \right)^{n} \right] . \tag{20}$$

Here m and n are positive integers, and in order to ensure thermodynamic stability it is assumed that $m > n$. The constants σ and ε define the potential's length and energy scales, respectively, and the normalization used in Eq. (20) ensures that the minimum pair potential energy is $-\varepsilon$ and that this value is obtained at $r = \sigma$. Note that the normalization is different from that usually employed for the standard 12-6 LJ pair potential parametrized as $4\varepsilon \left[(r/\sigma)^{-12} - (r/\sigma)^{-6} \right]$.

The aim of our study is to investigate whether any relation between the correlation coefficient and the density-scaling exponent can be determined. This involves simulating several state points for which the virial potential-energy correlations are not strong. With this goal in mind, a particular case of the generalized LJ potential was simulated, the case where $m = 2n$:

$$v_{2n,n}^{\mathrm{LJ}}(r) = \varepsilon \left[\left(\frac{\sigma}{r} \right)^{2n} - 2 \left(\frac{\sigma}{r} \right)^{n} \right] . \tag{21}$$

The following four instances of this pair potential, henceforth denoted by LJ(2n,n), were simulated in three dimensions: $n = 4, n = 9, n = 12$ and $n = 18$ (the $n = 6$ case corresponding to the standard LJ potential is considered later). Figure 1 shows that these four pair potentials are quite different as functions of the pairwise distance r.

The simulations were performed in the NVT ensemble, i.e., for a constant number of particles ($N = 864$) at constant temperature T and constant volume V. The time step was 0.001 (in LJ units) and the simulations were performed with periodic boundary conditions and a standard shifted potential cut-off at 2.5σ. Using an FCC crystal as starting configuration, each system was equilibrated for $2 \cdot 10^{6}$ time steps before the collection of data began. After equilibration, the simulation ran for $50 \cdot 10^{6}$ time steps during which data were collected. For each of the four systems, six densities were considered, $\rho = 0.25, 0.50, 0.75, 1.00, 1.25, 1.50$ (in LJ units); the temperature was varied
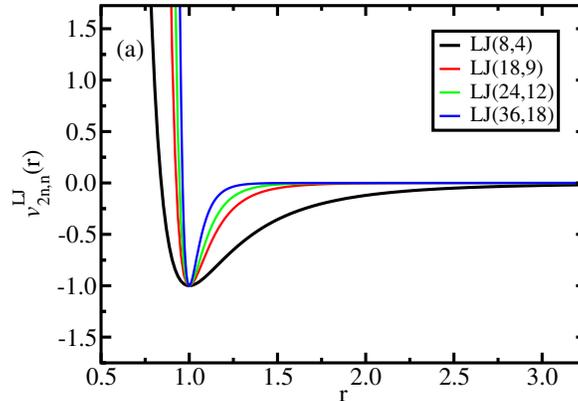
FIG. 1. The simulated four generalized Lennard-Jones (LJ) pair potentials of Eq. (21) plotted as a function of the pairwise distance r (distance and energy are given in LJ units): $n = 4$ (black), $n = 9$ (red), $n = 12$ (green), and $n = 18$ (blue). The potentials are quite different.

within the range $0.25 < T < 5.00$. At each state point the correlation coefficient and the density-scaling exponent were calculated from Eq. (1) and Eq. (16), respectively.

What to expect for the behavior of R when density is lowered? To answer this question we refer to the isomorph theory, which works well for the LJ and related pair potentials in the ordinary liquid phase. According to isomorph theory, if a reference state point (ρ_0, T_0) and another state point (ρ, T) are on the same isomorph, the ratio between T and T_0 defines what may be termed the isomorph shape function $h(\rho, S_{\text{ex}})$ via $T/T_0 = h(\rho, S_{\text{ex}})$ [23]. Thus each isomorph is mapped out in the phase diagram by

$$\frac{h(\rho, S_{\text{ex}})}{T} = \text{Const.} \tag{22}$$

The original isomorph theory predicted the function $h(\rho, S_{\text{ex}})$ to be independent of S_{ex}, whereas the more correct theory from 2014 predicts that h may vary slightly from isomorph to isomorph [14]. In both cases, however, the analytical form of the density dependence is the same. For the LJ$(2n, n)$ pair potential it can be shown that the shape function takes the following form in d dimensions [14, 23–25]

$$h(\rho, S_{\text{ex}}) = \left(\frac{d}{n}\gamma_0 - 1\right)\left(\frac{\rho}{\rho_0}\right)^{2n/d} - \left(\frac{d}{n}\gamma_0 - 2\right)\left(\frac{\rho}{\rho_0}\right)^{n/d}. \tag{23}$$

Here (ρ_0, T_0) is the isomorph reference state point, at which γ_0 is the density-scaling exponent – the S_{ex} (isomorph) dependence of the function h is contained in γ_0. Combining Eqs. (22) and (23) one can map out an isomorph from information obtained by computer simulations at the reference state point, i.e., with no need to use Eq. (17) in a tedious step-by-step process.

Note that Eq. (22) and the definition of the density-scaling exponent Eq. (17) implies [26]

$$\gamma = \frac{d\ln h}{d\ln \rho}. \tag{24}$$

Thus when the density-scaling exponent is known at a single reference state point, the theory via Eq. (23) and Eq. (24) predicts how γ varies with density along the isomorph in question.

In Eq. (23) there are two terms, one positive and one negative. At high densities the positive term dominates. Upon lowering the density, $h(\rho, S_{\text{ex}})$ changes sign when the negative term dominates. This implies negative isomorph temperatures, compare Eq. (22), implying that the isomorph theory must break down. Since the theory works well when there are strong virial potential-energy correlations, one concludes that the correlation coefficient must decrease upon lowering density along a configurational adiabat, i.e., for generalized LJ systems in any dimension the isomorph theory predicts its own breakdown at sufficiently low densities.

LJ(8,4) LJ(18,9)
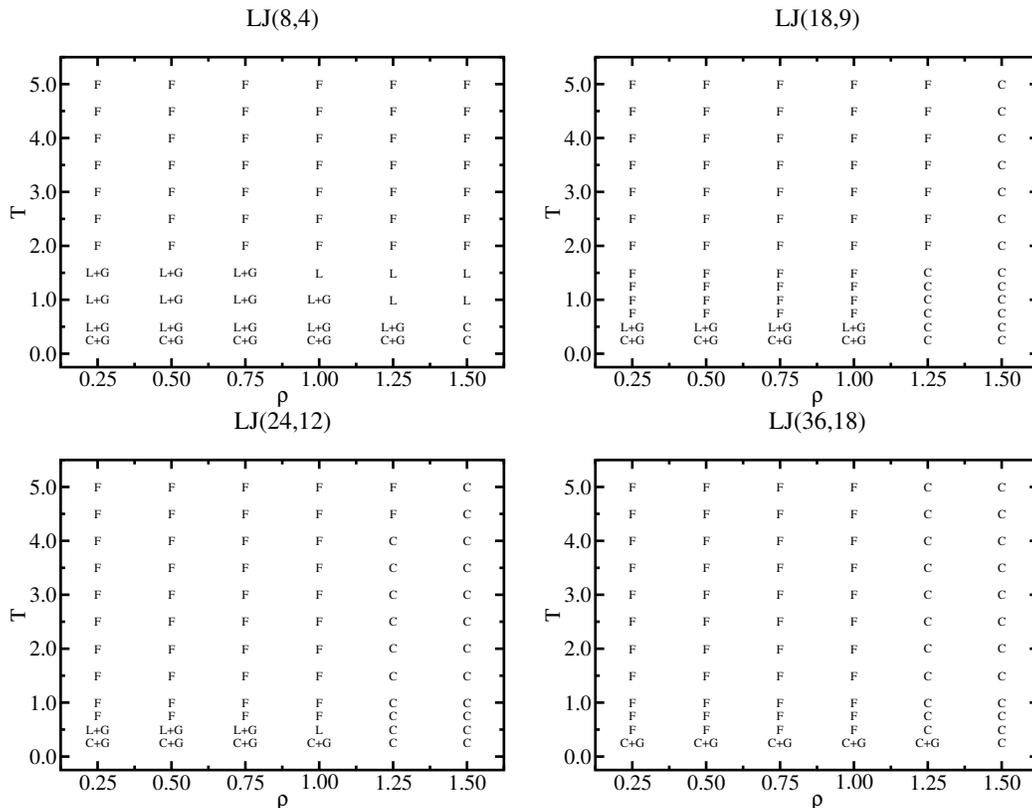
LJ(24,12) LJ(36,18)

FIG. 2. State points simulated for the pair potentials LJ(8,4), LJ(18,9), LJ(24,12), LJ(36,18) defined by Eq. (21). At each state point the virial potential-energy correlation coefficient (Eq. (1)) and the density-scaling exponent (Eq. (16)) was evaluated. Most state points are at supercritical temperatures (at which the liquid and gas phases merge) and marked by an F – F means fluid, L means liquid, C means crystalline, L+G means a state point of coexisting liquid and gas phases, etc. The phases were identified by visual inspection.

To summarize, moving along a given isomorph it is possible to define a lower density limit beyond which the isomorph theory does not hold. The condition that the shape function is non-negative sets the following limit for the isomorph theory to work:

$$\rho > \left(\frac{d\gamma_0 - 2n}{d\gamma_0 - n} \right)^{d/n} \rho_0 \,. \tag{25}$$

We have seen that R decreases as density is lowered along a configurational adiabat (isomorph). Moreover, according to Eq. (16) the scaling exponent must approach zero if $R \to 0$. Since $R = 0$ implies $\gamma = 0$, one expects that γ also decreases upon lowering the density. If density is increased, on the other hand, the positive term of Eq. (23) dominates and the density-scaling exponent eventually approaches $2n/d$ due to dominance of the repulsive r^{-2n} term [23–25]. At the same time R tends to unity. After considering these two limits, we turn to the simulation results.

Figure 2 shows the state points studied, marking in each case whether it is a solid or liquid state point, etc. Most state points are supercritical in which case we marked them by an F indicating "fluid". Figure 3 plots γ versus R along the isochores and isotherms for the four generalized LJ$(2n,n)$ potentials. Our findings are consistent with the theoretically predicted result that as $R \to 1$, γ approaches the high-density limiting values 8/3, 6, 8, and 12, respectively, although we never come close to these values, applying whenever the attractive term of the potential may be ignored. The density-scaling exponent changes behavior and starts to decrease with increasing R in the region where R is around 0.9 which, as mentioned earlier, is the threshold usually used to define R simple systems. In the opposite limit $R \to 0$ we find as expected $\gamma \to 0$.

Our data show that the change of behavior in γ versus R takes place at the boundary to the region in which the system is R simple. A more extensive study is needed to determine whether this holds also for other R simple systems. If confirmed, the relation between the change in the behavior of the density-scaling exponent and the value of the correlation coefficient could be useful in practice, because R is not accessible in experiment while γ is [27]. A change
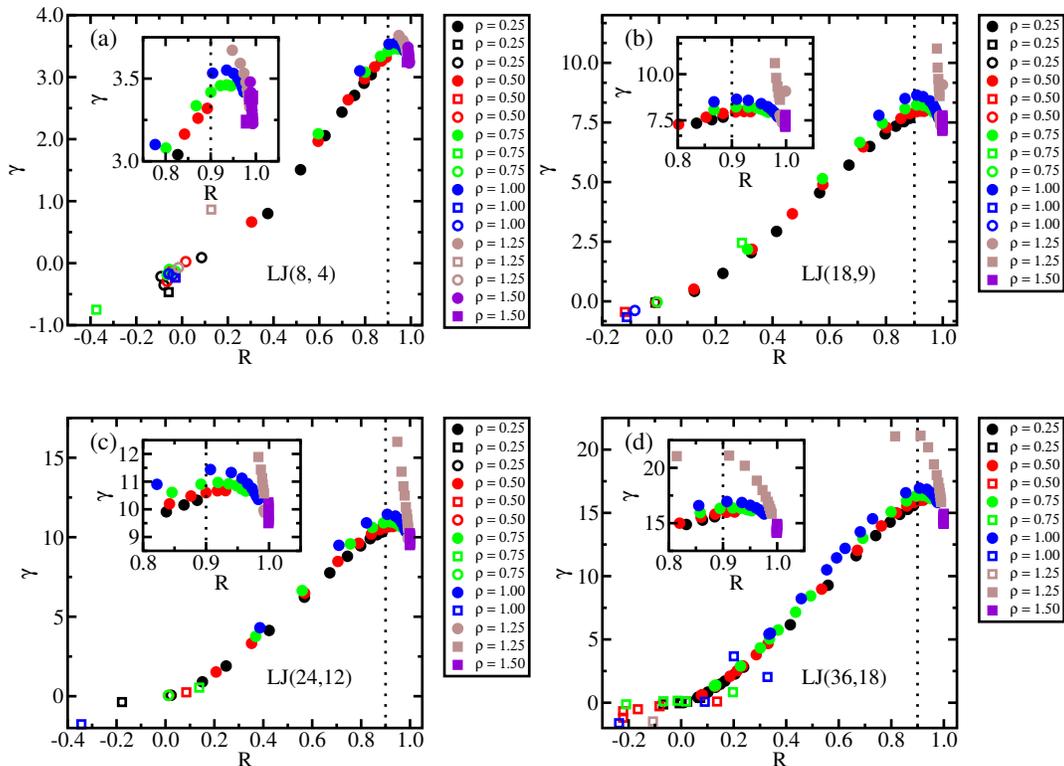
FIG. 3. The density-scaling exponent, γ, versus the correlation coefficient, R, for generalized LJ potentials: (a) LJ(8,4); (b) LJ(18,9); (c) LJ(24,12); (d) LJ(36,18). Full squares mark crystalline states, full circles are liquid, fluid, or gas states – open squares are coexisting crystal-gas states; open circles are coexisting liquid-gas states. The simulated state points are given in Fig. 2. The inset in each figure focuses on the crossover region. Along each isochore the temperature was varied in the range $0.25 < T < 5.00$. In (b), (c), and (d) it is possible to distinguish two different behaviors of the variation of γ with R, which reflects liquid contra crystal phases (the latter being the steepest). The state points with negative or close to zero correlation coefficient are all in the gas-liquid coexistence region.

in the density or temperature dependence of γ might therefore be used for identifying in which regions of the phase diagram a liquid is expected to obey isomorph theory predictions like isochronal superposition, excess entropy scaling, etc [7].

Figure 4 summarizes the data of Fig. 3. There is a roughly linear behavior between γ and R, but it does not extend above $R \approx 0.9$ where γ as mentioned starts to decrease towards the value $2n/3$ predicted at high density (where the r^{-2n} repulsive term dominates and the virial potential-energy correlations become virtually perfect). For $R > 0.9$ the system is R simple and the density variation of γ is well described by Eqs. (23) and (24). For this reason we henceforth focus on the region in which $R < 0.9$.

Figure 4(b) plots the data differently and establishes for most of the $R < 0.9$ data the following approximate proportionality:

$$\gamma/n \simeq R \,. \tag{26}$$

How to understand this? In Ref. 2 it was shown that an LJ-type pair potential may be approximated by the "extended inverse power law (eIPL)" pair potential with an effective state-point-dependent exponent p that is *not* simply the exponent of the repulsive term of the LJ-type potential:

$$v(r) \cong Ar^{-p} + B + Cr \,. \tag{27}$$

This approximation usually works very well within the entire first coordination shell [2]. At typical condensed-matter low and moderate pressure state points the term $B + Cr$ contributes little to the forces on a given particle, because
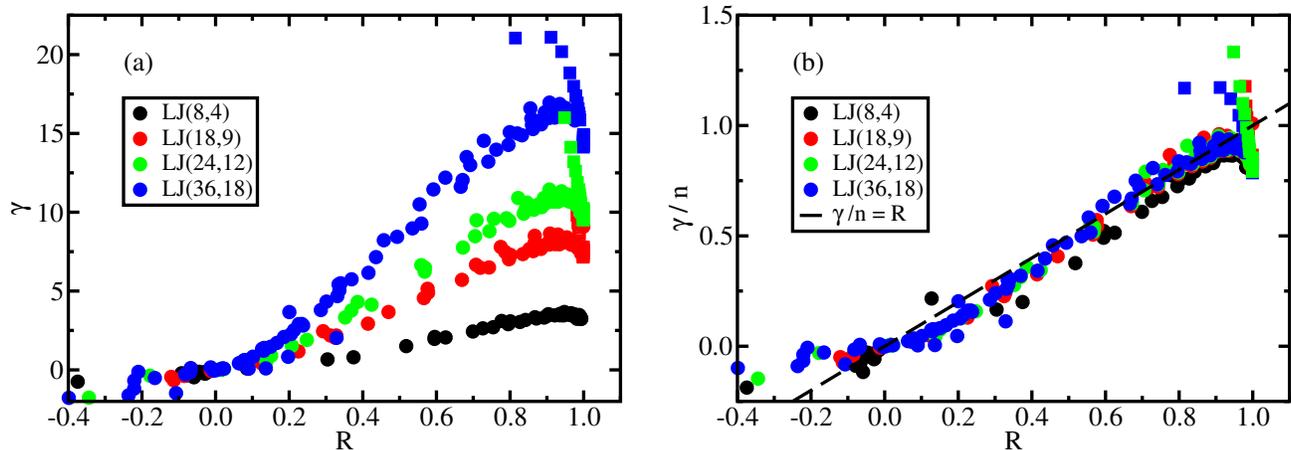
FIG. 4. (a) All data of Fig. 3 in a common plot in which squares are crystalline states, circles are liquid, fluid, or gas states. (b) The same data with γ/n plotted versus R. The black dashed line connects the points $(0,0)$ with $(1,1)$, demonstrating the universal, roughly linear dependence Eq. (26). Significant deviations from this are seen mainly for $R > 0.9$ and for $R < 0$. The former case refers to the R simple region of the phase diagram, the latter to states of coexisting liquid and gas phases (compare Fig. 2).

the sum of these terms over all nearest neighbors tends to be almost constant. This reflects the fact that if the particle is moved slightly, some nearest-neighbor distances increase and some decrease, but their sum stays almost constant [2]. This implies that the total force contribution from the $B + Cr$ term is small and the physics is dominated by the r^{-p} IPL term.

For an IPL pair potential $\propto r^{-p}$ the density-scaling exponent is given in d dimensions by [2]

$$\gamma = \frac{p}{d}. \tag{28}$$

As mentioned, the effective exponent p of Eq. (27) varies with state point. In large parts of the phase diagram of the generalized LJ pair potential the effective exponent p is considerably larger than m [2]. This is because even within the repulsive *part* of the pair potential, i.e., at distances below the potential minimum, there is a sizable contribution from the attractive r^{-k} *term* making the repulsions significantly steeper than expected from the r^{-m} repulsive term alone. At densities and temperatures dominated by the pair potential minimum, i.e., at typical low or moderate pressure condensed-matter state points, it may be shown from a curvature argument referring to the potential-energy minimum that the effective exponent of the generalized LJ pair potential Eq. (20) is given [2] by

$$p = m + n. \tag{29}$$

At sufficiently high density and/or temperature the repulsive r^{-m} term dominates the physics, however, and here one finds that $p \to m$. These conditions arise as $R \to 1$.

For the standard LJ pair potential at typical state points the density-scaling exponent is between 5 and 6, corresponding via Eq. (28) to p between 15 and 18 [1, 2]. Based on the above we expect that the LJ(2n,n) pair potential in a large part of its phase diagram is equivalent to an eIPL pair potential with $p \simeq 2n + n = 3n$. Via Eq. (28), this corresponds in three dimensions to

$$\gamma \simeq n. \tag{30}$$

In summary, $R \to 1$ at state points of large density and/or temperature where the r^{-2n} term dominates the physics. This behavior is hinted at in Fig. 4(b) above $R \simeq 0.9$ where γ/n starts to decrease and systematically deviates from the red dashed line. The limit $\gamma \simeq 2n/3$ was not reached in our simulations, however, which shows that only at *very* high density or temperature the attractive term of the generalized LJ pair potential may be ignored. A linear extrapolation of most of the data to $R = 1$ gives the limit value suggested by the eIPL approximation in conjunction

with Eq. (29). We take this as an indication that the eIPL approximation works well at the state points simulated, whether or not these are characterized by strong virial potential-energy correlations.

Having identified the limits $\gamma \to 0$ for $R \to 0$ and $\gamma \to n$ for $R \to 1$ (as long as $R < 0.9$, i.e., for most data), the next question one may ask is: why do the data follow the approximate linear relation Eq. (26)? A possible explanation refers again to the eIPL approximation. The virial is calculated in d dimensions from the pair potential as a sum over terms of the form $rv'(r)/d$ [1]. For the eIPL pair potential Eq. (27) this gives Apr^{-p}/d plus an approximate constant (compare the above argument). Thus for fluctuations away from the equilibrium value, if the linear term of Eq. (27) is uncorrelated to the IPL term, the eIPL approximation suggests that one may have effectively

$$\Delta W \simeq (p/d)\Delta U \qquad (31)$$

with $p \cong 3n$ for $d = 3$. This must be, admittedly, a very rough approximation when the W U correlations are not strong, but if one does make it, Eq. (1) and Eq. (16) imply

$$\gamma/R \simeq \sqrt{\langle(\Delta W)^2\rangle}/\sqrt{\langle(\Delta U)^2\rangle} \simeq p/d \simeq n \,. \qquad (32)$$

This is Eq. (26) that summarizes our findings for most state points in three dimensions. A simple way of expressing this is that the exponent γ_2 of Eq. (18) is roughly constant throughout the phase diagram, compare Eq. (19).

B. The Lennard-Jones pair potential in two, three, and four dimensions

We proceed to report results for the standard LJ system in two, three, and four dimensions. Details on how the simulations were performed can be found in Refs. 25 and 28. Figure 5(a) shows the density-scaling exponent versus the correlation coefficient along three configurational adiabats in the liquid phase and two in the crystalline phase for the two-dimensional LJ system; (b) shows a similar plot along two configurational adiabats in the liquid phase of the three-dimensional LJ system.
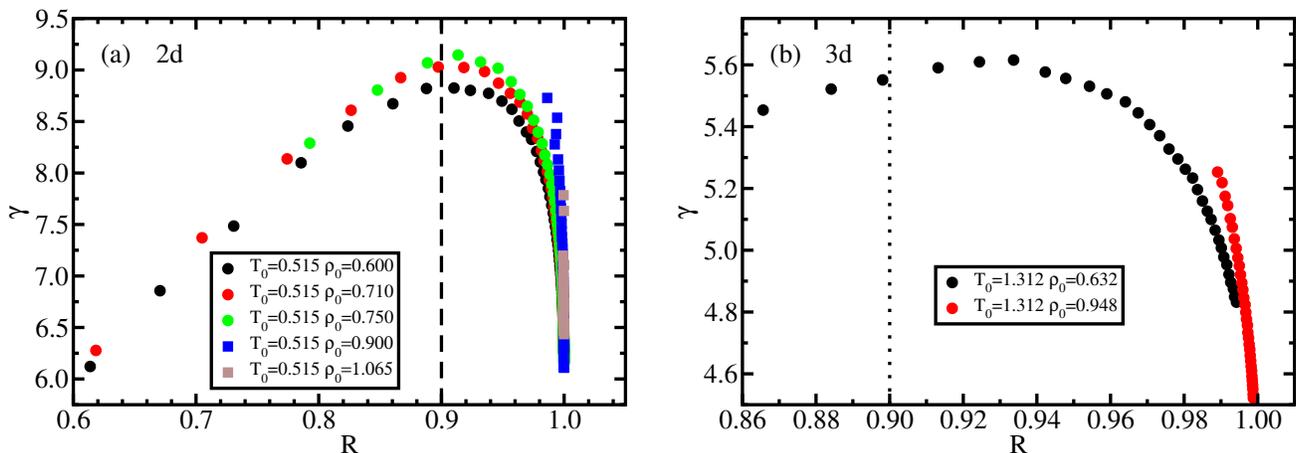
FIG. 5. The density-scaling exponent, γ, versus the correlation coefficient, R, along configurational adiabats in two and three dimensions with insets giving the reference state points. (a) Results for three configurational adiabats in the liquid phase and two in the crystalline phase generated using Eq. (17) for the $2d$ LJ system. The density-scaling exponent increases with increasing R for values of R below the 0.9 threshold and then starts to decrease. For the crystalline phase R is always larger than 0.9 and γ decreases with increasing R (towards $12/2 = 6$). (b) Two configurational adiabats for the liquid phase of the $3d$ LJ system, constructed as in the $2d$ case. The decrease in γ starts a bit after the 0.9 threshold.

Figure 6 shows the density-scaling exponent versus the correlation coefficient along the configurational adiabats defined by the critical points for the LJ system in two, three, and four dimensions. Data for the critical points are taken from Refs. 29–31. For the configurational adiabats in the liquid phase the relation between R crossing the threshold value 0.9 and the start of the decreasing behavior of γ is observed. For the crystalline phase, the correlation coefficient is above 0.9 for all the state points studied and no crossover is observed.
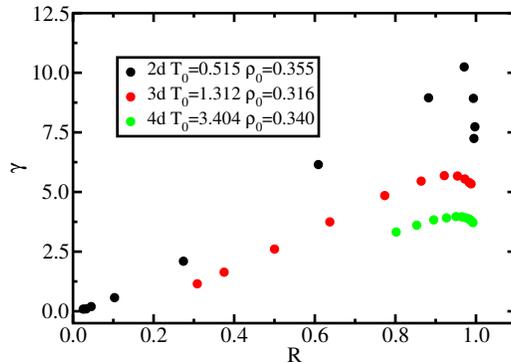
FIG. 6. The density-scaling exponent, γ, versus the correlation coefficient, R, along configurational adiabats with reference state points (inset) equal to the critical points of the LJ system in two, three, and four dimensions. In all cases, γ exhibits a maximum in the region where the correlation coefficient crosses the threshold value $R = 0.9$. Note that the maximum value of γ decreases with increasing dimension.

In d dimensions the eIPL-justified relation Eq. (32) implies via $p = 2n + n = 3n$ that

$$\gamma\, d \cong 3\, n\, R\,. \tag{33}$$

This is tested in Fig. 7(a) for the LJ simulations in $2 - 4$ dimensions. We see that Eq. (33) overall works well.

Figure 7(b) tests all data of the paper versus Eq. (33). The data in the region where the system is not R simple conforms roughly to Eq. (33), unless $R < 0$ which are state points of liquid-gas coexistence.
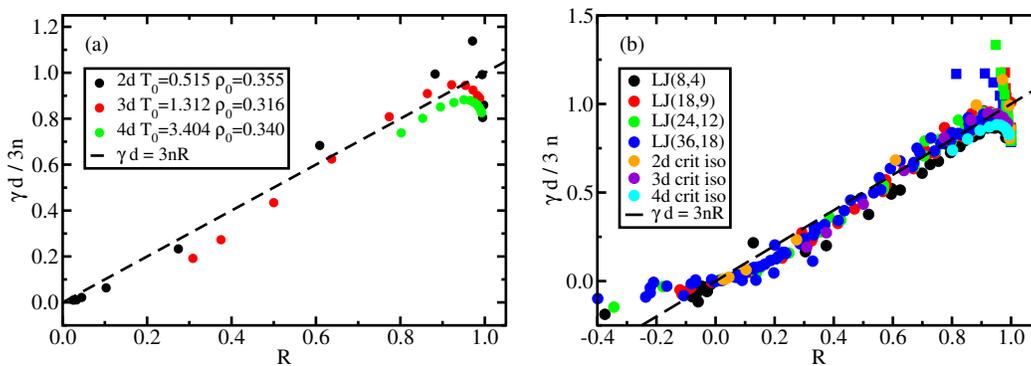
FIG. 7. Normalized density-scaling exponent versus the potential-energy correlation coefficient with squares marking crystalline states and spheres marking liquid, fluid, or gas states. (a) The data for the LJ system in two, three, and four dimensions. (b) All data of the paper, demonstrating the approximate linear relationship Eq. (33) below $R \approx 0.9$ (dashed line). Above this value there is a different behavior as discussed in the text.

IV. CONCLUSIONS

For the state points where the system is not R simple ($R < 0.9$) the generalized Lennard-Jones systems have a roughly linear relation between the density-scaling exponent and the virial potential-energy correlation coefficient of Eq. (33) (unless $R < 0$ corresponding to liquid-gas coexistence state points). This finding has been rationalized in terms of the extended inverse-power-law approximation. Above $R \cong 0.9$ the approximate linear relation $\gamma \propto R$ breaks down, however, and when R approaches unity the density-scaling exponent starts to decrease in its variation with R. γ is expected to eventually obey $\gamma \to 2n/d$ as $R \to 1$ when the repulsive r^{-2n} term dominates completely. This happens only at very large densities and/or temperatures, however.

Our numerical data show that the threshold value $R \cong 0.9$ has a hitherto not recognized significance. While it was previously known that this threshold characterizes the state points for which the isomorph theory works well [4, 7], it is a new finding that roughly the same threshold marks a crossover from the $\gamma \propto R$ behavior found for $R < 0.9$ to one of decreasing γ with increasing R. It would be interesting to find out how general the finding of a threshold at $R \cong 0.9$ is. If it is general, this opens for the possibility that determining the experimental variation of the density-scaling exponent throughout the phase diagram may be used for determining where the system in question is R simple and where it is not.

[1] Nicholas P. Bailey and Ulf R. Pedersen and Nicoletta Gnan and Thomas B. Schrøder and Jeppe C. Dyre, "Pressure-energy correlations in liquids. I. Results from computer simulations," Journal of Chemical Physics **129**, 184507 (2008).

[2] Nicholas P. Bailey and Ulf R. Pedersen and Nicoletta Gnan and Thomas B. Schrøder and Jeppe C. Dyre, "Pressure-energy correlations in liquids. II. Analysis and consequences," Journal of Chemical Physics **129**, 184508 (2008).

[3] Thomas B. Schrøder and Nicholas P. Bailey and Ulf R. Pedersen and Nicoletta Gnan and Jeppe C. Dyre, "Pressure-energy correlations in liquids. III. Statistical mechanics and thermodynamics of liquids with hidden scale invariance," Journal of Chemical Physics **131**, 234503 (2009).

[4] Nicoletta Gnan and Thomas B. Schrøder and Ulf R. Pedersen and Nicholas P. Bailey and Jeppe C. Dyre, "Pressure-energy correlations in liquids. IV. 'Isomorphs' in liquid state diagrams," Journal of Chemical Physics **131**, 234504 (2009).

[5] Thomas B. Schrøder and Nicoletta Gnan and Ulf R. Pedersen and Nicholas Bailey and Jeppe C. Dyre, "Pressure-energy correlations in liquids. V. Isomorphs in generalized Lennard-Jones systems," Journal of Chemical Physics **134**, 164505 (2011).

[6] Trond S. Ingebrigtsen and Thomas B. Schrøder and Jeppe C. Dyre, "What is a simple liquid?" Physical Review X **2**, 011011 (2012).

[7] Jeppe C. Dyre, "Hidden Scale Invariance in Condensed Matter," The Journal of Physical Chemistry B **118**, 10007 (2014).

[8] Jeppe C. Dyre, "Simple liquids' quasiuniversality and the hard-sphere paradigm," J. Phys.: Condens. Matter **28**, 323001 (2016).

[9] A. Malins, J. Eggers, and C. P. Royall, "Investigating Isomorphs with the Topological Cluster Classification," J. Chem. Phys. **139**, 234505 (2013).

[10] E. H. Abramson, "Viscosity of fluid nitrogen to pressures of 10 GPa," J. Phys. Chem. B **118**, 11792–11796 (2014).

[11] J. Fernandez and E. R. Lopez, "in Experimental Thermodynamics: Advances in Transport Properties of Fluids," (Royal Society of Chemistry, 2014) Chap. 9.3, pp. 307–317.

[12] E. Flenner, H. Staley, and G. Szamel, "Universal Features of Dynamic Heterogeneity in Supercooled Liquids," Phys. Rev. Lett. **112**, 097801 (2014).

[13] S. Prasad and C. Chakravarty, "Onset of Simple Liquid Behaviour in Modified Water Models," J. Chem. Phys. **140**, 164501 (2014).

[14] Schrøder, Thomas B. and Dyre, Jeppe C., "Simplicity of condensed matter at its core: Generic definition of a Roskilde-simple system," Journal of Chemical Physics **141**, 204502 (2014).

[15] U. Buchenau, "Thermodynamics and dynamics of the inherent states at the glass transition," J. Non-Cryst. Solids **407**, 179–183 (2015).

[16] K. R. Harris and M. Kanakubo, "Self-diffusion, velocity cross-correlation, distinct diffusion and resistance coefficients of the ionic liquid [BMIM][Tf2N] at high pressure," Phys. Chem. Chem. Phys. **17**, 23977–23993 (2015).

[17] D. M. Heyes, D. Dini, and A. C. Branka, "Scaling of Lennard-Jones liquid elastic moduli, viscoelasticity and other properties along fluid-solid coexistence," Phys. Status Solidi (b) **252**, 1514–1525 (2015).

[18] Walter Schirmacher, Giancarlo Ruocco, and Valerio Mazzone, "Heterogeneous viscoelasticity: A combined theory of dynamic and elastic heterogeneity," Phys. Rev. Lett. **115**, 015901 (2015).

[19] C. M. Roland, S. Hensel-Bielowka, M. Paluch, and R. Casalini, "Supercooled Dynamics of Glass-Forming Liquids and Polymers under Hydrostatic Pressure," Rep. Prog. Phys. **68**, 1405–1478 (2005).

[20] J.-P. Hansen and I. R. McDonald, *Theory of Simple Liquids: With Applications to Soft Matter*, 4th ed. (Academic, New York, 2013).

[21] Yaakov Rosenfeld, "A quasi-universal scaling law for atomic transport in simple fluids," Journal of Physics: Condensed Matter **11**, 5415 (1999).

[22] L.D. Landau and E.M. Lifshitz, *Statistical Physics*, edited by Oxford (Pergamon, 1958).

[23] L. Bøhling and T. S. Ingebrigtsen and A. Grzybowski and M. Paluch and J. C. Dyre and T. B. Schrøder, "Scaling of viscous dynamics in simple liquids: theory, simulation and experiment," New J. Phys. **14**, 113035 (2012).

[24] Trond S. Ingebrigtsen and Lasse Bøhling and Thomas B. Schrøder and Jeppe C. Dyre, "Thermodynamics of condensed matter with strong pressure-energy correlations," Journal of Chemical Physics **136**, 061102 (2012).

[25] Lorenzo Costigliola, *Isomorph theory and extensions*, Ph.D. thesis, Roskilde Universitet (2016).

[26] T. S. Ingebrigtsen, L. Bøhling, T. B. Schrøder, and J. C. Dyre, "Thermodynamics of Condensed Matter with Strong Pressure-Energy Correlations," J. Chem. Phys. **136**, 061102 (2012).

[27] Ditte Gundermann, Ulf R. Pedersen, Tina Hecksher, Nicholas P. Bailey, Bo Jakobsen, Tage Christensen, Niels B. Olsen, Thomas B. Schroder, Daniel Fragiadakis, Riccardo Casalini, C. Michael Roland, Jeppe C. Dyre, and Kristine Niss, "Predicting the density-scaling exponent of a glass-forming liquid from Prigogine-Defay ratio measurements," Nat. Phys. **7**, 816.

[28] Lorenzo Costigliola, Thomas B. Schrøder and Jeppe C. Dyre, "Communication: Studies of the Lennard-Jones fluid in 2, 3, and 4 dimensions highlight the need for a liquid-state 1/d expansion," The Journal of Chemical Physics **144**, 231101 (2016).

[29] Smit, B. and Frenkel, D., "Vapor-liquid equilibria of the two-dimensional Lennard-Jones fluid(s)," The Journal of Chemical Physics **94**, 5663 (1991).

[30] Potoff, Jeffrey J. and Panagiotopoulos, Athanassios Z., "Critical point and phase behavior of the pure fluid and a Lennard-Jones mixture," The Journal of Chemical Physics **109**, 10914 (1998).

[31] Hloucha, M. and Sandler, S. I., "Phase diagram of the four-dimensional Lennard-Jones fluid," The Journal of Chemical Physics **111**, 8043–8047 (1999).